Development of a Finite Element Model for the Load Rating of Temporary Railcar Bridges

NCDOT Project TA2025-12
FHWA/NC/TA202025-12
December 2025

Vikita Kamala, Taylor Brodbeck, and Ghadir Haikal
Department of Civil, Construction, and Environmental Engineering, North Carolina State University

RESEARCH & DEVELOPMENT

Development of a Finite Element Model for the Load Rating of Temporary Railcar Bridges

FINAL REPORT

Submitted to:
North Carolina Department of Transportation
Research and Development Unit
(Research Project No. TA2025-12)

Submitted by

Vikita Kamala, Taylor Brodbeck, and Ghadir Haikal
Department of Civil, Construction, and Environmental Engineering, North Carolina State University
915 Partners Way, Campus Box 7908, Raleigh NC 27606
919-515-7823
ghaikal@ncsu.edu

North Carolina State University

December 2025

Technical Report Documentation Page

1. **Report No.** FHWA/NC/TA202025-12	2. **Government Accession No**.	3. **Recipient's Catalog No**.
4. **Title and Subtitle** Development of a Finite Element Model for the Load Rating of Temporary Railcar Bridges		5. **Report Date** 12/31/2025 6. **Performing Organization Code**
7. **Author(s)** Vikita Kamala, Taylor Brodbeck, and Ghadir Haikal		8. **Performing Organization Report No.**
9. **Performing Organization Name and Address** Vikita Kamala, https://orcid.org/0009-0002-3727-1325 Taylor Brodbeck, https://orcid.org/0009-0007-9543-1610 Ghadir Haikal, https://orcid.org/0000-0001-9628-7621		10. **Work Unit No. (TRAIS)** 11. **Contract or Grant No**.
12. **Sponsoring Agency Name and Address** North Carolina Department of Transportation Research and Development Unit 1549 Mail Service Center Raleigh, North Carolina 276699-1549		13. **Type of Report and Period Covered** 06/01/2025-12/31/2025 14. Sponsoring Agency Code TA2025-12
15. **Supplementary Notes**		

16. **Abstract**

Hurricane Helene (2024) caused massive destruction in Western North Carolina (WNC), rendering more than three dozen bridges in the state unfunctional. Many of these bridges were replaced by railroad flatcars (RRFC) as temporary bridges to resume routes to critical facilities like schools, hospitals etc. RRFC bridges are still currently in use in the WNC region, but the strength, capacity and response characteristics of these temporary structures are unknown. In the absence of literature and design specifications for temporary RRFC bridges, there is an immediate need to access the structural performance of these temporary structures for the purpose of load rating. This technical report details a computational approach to load rate temporary RRFC bridge structures. We develop a high-fidelity three-dimensional finite element model to simulate the response of a representative RRFC bridge under critical traffic loads. The model is validated using experimental data obtained through a parallel experimental study supported by the North Carolina Department of Transportation. The validated computational modeling methodology will be used to establish a reliable load rating procedure for RRFC bridges and set the stage for the implementation of design procedures for RRFC bridges as temporary structures in the state of North Carolina.

17. **Keywords** Railroad flatcar, temporary bridges, Load and rating factors, computational modeling, finite element analysis	18. **Distribution Statement**		
19. **Security Classif**. (of this report) unclassified	20. **Security Classif**. (of this page) unclassified	21. **No. of Pages** 29	22. **Price**

Form DOT F 1700.7 (8-72) **Reproduction of completed page authorized**

DISCLAIMER

The contents of this report reflect the views of the authors and are not necessarily the views of North Carolina State University. The authors are responsible for the facts and the accuracy of the data presented herein. The contents do not necessarily reflect the official views or policies of the North Carolina Department of Transportation at the time of publication. This report does not constitute a standard, specification, or regulation.

ACKNOWLEDGEMENTS

The authors would like to thank the North Carolina Department of Transportation (NCDOT) for the funding of this investigation and access to Swannanoa bridge for experimental testing. Special thanks to Mr. David Snoke, P.E., State Structures Engineer for the NCDOT for patiently answering the questions from our research team. The authors would like to thank the Swannanoa Fire Department for providing the emergency vehicle and personnel to help with the experimental testing of the Swannanoa bridge.

Additionally, the authors would like to acknowledge and express gratitude for the contribution of Dr. Gregory Lucier and his team at the Construction Facilities Laboratory, Mr. Johnathan McEntire, Ms. Allison Ebbert and Mr. Russell Barry at NCSU, for organizing and carrying out experimental testing of the Swannanoa bridge and providing the crucial data required for model validation.

EXECUTIVE SUMMARY

Hurricane Helene (2024) caused substantial loss of life, property and massive destruction of infrastructure in the Western North Carolina (WNC), including damage to hundreds of bridges and thousands of miles of road. Immediate restoration of crucial routes serving hospitals, medical supply industries, and other essential facilities necessitated rapid repair/ replacement of these damages bridges. Many of these bridges were replaced by temporary structures fashioned by propping railroad flatcars (RRFC) as bridge decks. Replacement of these temporary structures with permanent ones will take years, thus many of these temporary bridges are still functional in the WNC.

Standard structural analysis and load rating procedures cannot be used to estimate structural response and estimate capacities of these RRFC bridges owing to their unconventional geometry. Available literature on load RRFC of bridges mainly focuses on permanent bridges with composite concrete deck, and can therefore not be applied to these temporary structures. In this technical report we detail a computational approach to investigate the structural response of RRFC temporary bridges with the aim of developing a load rating methodology to estimate safe traffic loads for these structures.

For a representative RRFC bridge, we build a finite element model in section Chapter 2. The model is validated using data from an on-field experiment conducted by Dr. Lucier's team. Having established model fidelity, we use the model to analyze the response of RRFC structure to the traffic load of an emergency vehicle (EV3 per NC legal loads).

Given that the geometry of RRFC bridges changes considerably along the span, conventional analysis methods would be too conservative to compute capacity. Furthermore, conventional methods divide the bridge into strips along its width and analyzes each strip individually to simplify analysis. This assumption underestimates structure capacity since it does not consider the combined resistance of the bridge as a whole. Recommendations based on these results can thus lead to expensive repair/ upgrade.

Alternatively, having a 3D model, we develop and detail procedures to compute demand and capacity at various sections along the span. These computations account for the actual geometry at each particular section without the simplifying assumptions that lead to conservative results. Load Rating Factors (LFR) are computed at each section using shear and moment envelopes. Comparison of capacity and demand shows that the representative example picked here can safely carry the load of an EV2, but is not recommended to carry EV3 vehicles.

TABLE OF CONTENTS

LIST OF FIGURES

LIST OF TABLES

Chapter 1. Introduction

Hurricane Helene (2024) caused massive destruction in the Western North Carolina (WNC) regions with significant loss to life, livestock, property, and infrastructure, including water, sewage, power, and transportation networks. More than 6,000 miles of roads and hundreds of bridges were damaged ([1]). Bridges connecting crucial facilities like schools, hospitals, and industries producing and supplying medicines and other medical/surgical products were completely destroyed or rendered out of service. Immediate restoration of these routes was imperative for emergency responses and rehabilitation, which necessitated the rapid installation of temporary bridges constructed from flatbed railroad cars.

Figure 1 shows a railcar bridge located at Warren Wilson Rd. in Swannanoa, NC. Two railroad flatcar decks with 90-foot spans were welded side-by-side and placed over the abutments to fashion a temporary bridge structure. Figure 2 shows the underside of this bridge, where the structural members of the railroad flatcar decks can be seen. Each railroad flatcar consists of a central plate box girder braced

Figure 1: Railcar bridge at Warren Wilson Rd. in Swannanoa, NC

Figure 2*:* Refurbished railroad flatcar deck structural elements

laterally by assemblies of channel and angle sections. Geometric properties such as girder depth and web thickness, as well as channel and angle section dimensions, vary along the bridge span, with certain locations exhibiting visible signs of corrosion damage. This configuration is fairly typical of railroad flatcar deck structures. Some variations exist in size, number, and placement of bracing elements, as well as in the number of railcars used across the bridge width. At least 33 temporary bridges currently exist in WNC that rely on railcars as primary structural elements. Maintaining the safety and functionality of these structures is necessary until permanent replacements are installed.

Railcar bridges are not amenable to standard design and load rating specifications due to their unconventional geometry. The large number of railcar bridges currently in use, and the variability in structural configurations pose significant challenges for field and/or laboratory testing. In the absence of detailed experimental data for each railcar bridge, computational modeling provides a convenient and cost-effective avenue to assess the structural performance of railcar bridges. Detailed physics-based computational models can adequately capture bridge geometry and composition, and provide full field displacement, stress, and strain distributions that can be used for overall structural assessment, as well as to identify local damage vulnerabilities such as stress concentrations. Researchers have explored using computational models to investigate the load-carrying capacity of railcar bridges, but the literature has so far focused on bridges with composite decks ([2], [3], [4]).

1.1. Objective and Scope

The goal of this Technical Assistance Request (TAR) is to conduct a computational investigation of the structural performance of railcar bridges for the purpose of load rating. A three-dimensional Finite Element Models (FEM) of a sample bridge is used to simulate bridge response under Emergency Vehicle (EV3) loading. Bridge geometry and structural components are incorporated in detail in the physics-based model,

and full-field displacement, stress, and strain data are analyzed to establish a reliable load rating procedures for temporary railroad flatcar bridge structures. The model is validated using experimental data collected by Dr. Gregory Lucier's team, as part of a parallel Technical Assistance Request (TAR) supported by the North Carolina Department of Transportation (NCDOT).

The two-car bridge on Warren Wilson Road in Swannanoa is chosen as the focus of this study. The shallow Swannanoa River basin at the bridge location provides easy access for measuring structural member dimensions as well as setting up instruments below the bridge for experimental data collection. The bridge's position in a low-traffic area and its proximity to a local fire station allow experimental testing for multiple emergency vehicle loadings. The results of this bridge model will serve as a proof-of-concept for applying the computational methodology developed in this work to other configurations of railcar bridges.

The scope of work in this TAR includes the following tasks:

- Obtaining on-site measurements of structural member dimensions and bridge configuration
- Building a detailed three-dimensional physics-based FEM model of the railcar bridge on Warren Wilson Road in Swannanoa
- Experimental validation of the FEM to establish model fidelity.
- Investigation of the representative bridge capacity for post-disaster loads and establishing a load rating procedure based on 3D analysis results.

Chapter 2. Literature Review Results

Very limited literature is available for the load rating of temporary RRFC bridges. The Departments of Transportation (DOT) in some states like Arkansas, Iowa and Indiana, which have significant numbers of RRFC bridges in rural areas, have investigated the performance of some permanent and temporary RRFC structures. However, most of these investigations focus on composite concrete deck bridges and are not applicable to the temporary steel RRFC decks in service in WNC.

An experimental and numerical study conducted by the Arkansas State University [12] led to the development of a finite element software for load rating of flatcar and boxcar railcar bridges in Arkansas. Experimental tests were performed on a one-third scale model of RRFC bridge. The developed software was shown to accurately predict load rate for flatcar bridges with no significant damage. For boxcar bridges and bridges that exhibited large damage, software could not predict the structural response and load rating accurately. A series of study performed at the Iowa State University [13-16] to develop load rating procedures and guidelines for selection of RRFC structures. This work highlighted the importance of various geometric characteristics of the elements of a RRFC structure like member straightness, member damage, structural element configuration, camber characteristics etc. Hence, considering the fact that the geometry and spans of bridges investigated in these studies are very different than the bridges in service in the WNC, it is important to perform structural assessments and develop load rating methodologies specifically for the temporary RRFC bridges in WNC.

Experimental and numerical studies carried out at Purdue University ([2-4], [8], [10]) lead to development of load rating methodology for RRFC bridges with composite decks. Experimentally validated numerical models were used to conduct parametric study with varying flatcar spacing, load positions and member stiffness. This work led to a better understanding of the RRFC bridge behavior. It is important to note that since these studies were focused on RRFC bridges with composite decks, their results cannot be applied directly to the RRFC bridges in WNC. This study, however, demonstrated the advantage of utilizing 3D finite element models to understand the behavior of structures with unconventional geometries like the RRFC.

Load rating is typically conducted using conventional two-dimensional (2D) analysis by dividing the bridge into strips along its width and analyzing each strip individually as a beam. Empirical factors are used to account for lateral load distribution. This approach simplifies the analysis, and was shown to be conservative, but it obscures the behavior of the bridge as one continuous structure. The conservative results can lead to higher load postings and ultimately expensive repair and upgrade recommendations. Three-dimensional (3D) analysis does not rely on these simplifying assumptions and better captures the overall response of the complete structure as one whole continuum. Moreover, contributions from non-structural elements, such as railings, can be better captured in 3D analyses. Studies have shown that 3D analysis led to higher bridge load ratings [17]. We thus take a 3D computational approach in this investigation to understand the behavior of the RRFC bridges in WNC and to develop a load rating methodology for the same.

Chapter 3. Computational Model Setup

3.1. Field Condition and Bridge Geometry

As seen in Figure 2, the Warren Wilson Road bridge in Swannanoa is comprised of two railroad flatcar decks placed side by side and welded to a jumper plate on top. The flatcar deck consists of a main plate box girder with a depth of about 30 inches depth assembled from web and flange plates with thicknesses varying between 3/8 and 3/4 inches along the bridge span. The girder tapers down near its supports, reaching a reduced depth of about
13 inches. Assemblies of channels and angle sections provide lateral bracing throughout the span. The spacing between these assemblies is about 54 inches at mid-span and varies near the support. Wide flange beams laterally brace the central girders near the supports. Upside-down channels, tubes and angles run along the span of the bridge, acting as stiffeners to the deck. A few odd stiffeners are occasionally observed connected to the webs of the central girder and those of the truck mount assemblies.

Two truck mount assemblies can be seen near each end of the bridge. The bridge is supported by retaining walls on each end with a support width of approximately 2 feet on either side. This configuration leads to a clear span of 83 feet 2 inches between the supports, which is almost 20 feet beyond the original design span of a flatcar as it was intended to be supported at the truck mounts.

All members are connected through welded connections. Member cross-sectional dimensions, thicknesses, lengths, etc., were measured as accurately as possible on site using traditional instruments like tape, ultrasonic thickness gauges, and calipers. It is important to note that the lack of original structural drawings and limited access to most members makes taking these measurements difficult, but the geometry of the bridge was replicated as closely as possible with reasonable engineering judgment when measurements were not possible or ambiguous.

The asphalt layer on the bridge was observed to be less than 2 inches deep, and the overall width of the bridge was measured at nearly 18 feet. Taking into account the presence of railings on both sides, the bridge width was assumed to be less than 18 feet, which corresponds to a single lane of traffic per (AASHTO) American Association of State Highway and Transportation Officials [5]. Thus, in the present work, the bridge is analyzed for one-way traffic. On site, traffic was alternated in both directions.

3.2. Bridge Computational Model

A detailed physics-based finite element model of the railcar bridge on Warren Wilson Road in Swannanoa was built in Abaqus 2023. The geometry of the bridge was replicated in full detail, including the deck, girder (longitudinal), and beam (transverse) elements based on the physical measurements collected in the field. The model was discretized using three-dimensional quadratic tetrahedron (C3D10) elements. While the geometry supports the use of shell elements, given the small member thickness, solid elements are preferred for accurately enforcing compatibility conditions at the welded connections, as well as for capturing full field stresses to identify potential damage locations. Tetrahedron elements were selected to better accommodate the complex geometries involved. A mesh convergence study was conducted to ensure a converged solution and maintain computational efficiency, leading to an average element size of 3 inches.

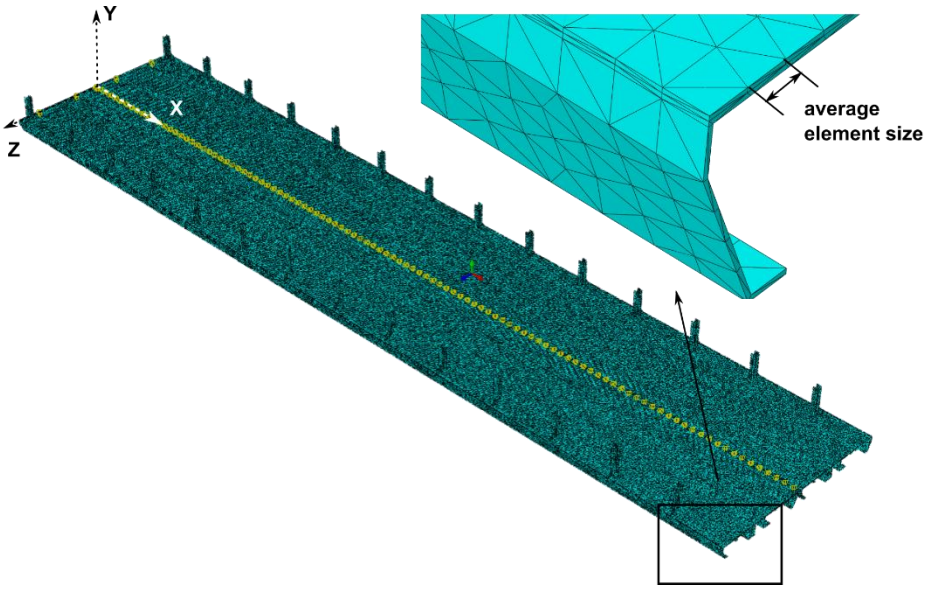

Figure 3: Mesh setup

The material properties for steel were determined based on testing conducted previously by WSP [6]. The tests reported a large variability in measured yield strength, hence a conservative yield strength of 36 ksi was selected for the preliminary analysis. Note that the yield strength is provided for reference only and to help identify potential yield locations, as the model assumed linear elasticity. In the absence of other elastic property measurements, a modulus of E = 30,0000 ksi was used, with Poisson's ratio ν = 0.26. Bridge self-weight was accounted for using a steel density value of 0.490 kcf (applied as mass density of 7.3e-4 lb⁄inch^3 with an acceleration of 386 in⁄sec^2) (AASHTO Design Table 3.5.1-1). Dead load equivalent to the 2 in asphalt layer (0.140 kcf per LRFD Design Table) was estimated at 0.168 lb⁄inch^2 and applied as pressure on the top surface of the bridge. Dead and live loads were applied separately to facilitate validation and load rating calculations.

The bridge boundary conditions were modeled by supporting the ends with roller supports over a 2 feet-wide bearing area at each end. The width of the support strip will be assessed in the field. Minimal lateral support was assumed to preclude rigid-body motion. This is a conservative setup that does now allow any uplift due to beam bending, which runs contrary to field observations. This assumption, however, significantly simplifies the modeling process, as incorporating the uplift conditions would require implementing a nonlinear contact model to track bridge movement and detect when the bottom surface comes into contact with the retaining wall. The effect of the boundary condition assumption can be explored in future efforts.

The analysis will be conducted using standard LRFD loading combinations, with live loads assuming a single NCDOT Emergency Vehicle for load rating purposes. Trucks will be modeled as moving loads to obtain moment and shear envelopes. Loads will be distributed to truck axles per NCDOT specifications, with wheel loads applied through 20"x10" rigid patches, as specified by AASHTO.

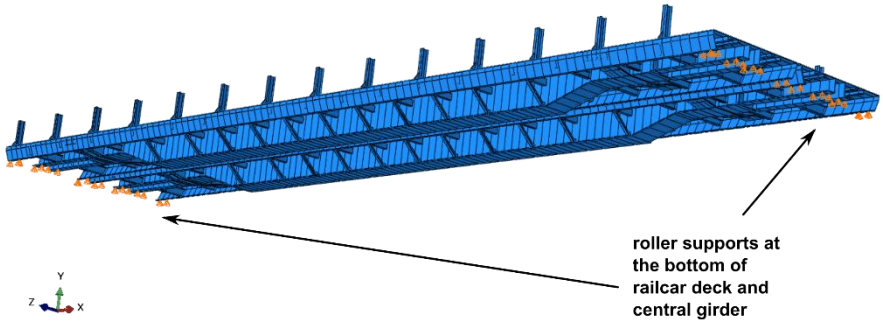

Figure 4: Boundary conditions simulating bridge resting on retaining wall

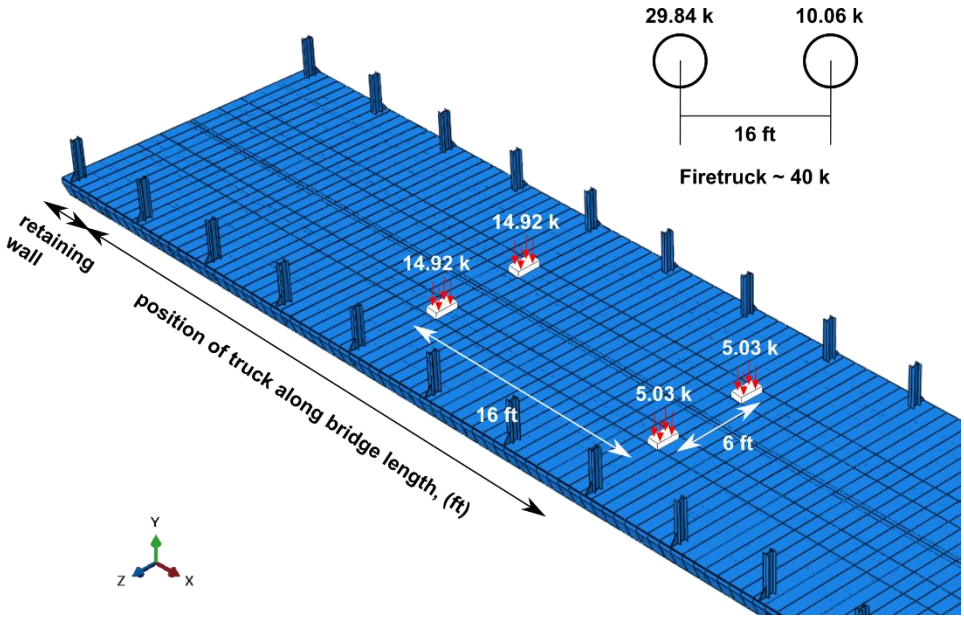

Figure 5: Load application: schematic representation of firetruck loads used for experimental validation

3.3. Experimental Validation

To establish model fidelity, we validate the Abaqus model using field test data collected as part of a parallel TAR effort led by Dr. Gregory Lucier [7]. In this test, a firetruck filled with 1500 gallons of water, weighing nearly
40 kips was driven across the Warren Wilson Road bridge in Swannanoa. The truck was stopped at intervals of approximately 10 ft along the bridge span. The truck position was measured as the distance between the bridge support and the front axle of the truck. Truck positions range from 0 to 70 ft as the truck moves from the west to the east end of the bridge. Deflection and strain measurements were collected at mid-span for each stop.

The loading sequence was replicated in the computational model. Axle loads were applied through rigid patches representing truck tires and were moved by 10 ft increments along the bridge span, as shown in Figure 5. The front and back axles weighed 10.06 kips and 29.84 kips, respectively. Each axle is represented

by two loading patches measuring 20 inches by 10 inches and spaced 6 ft apart. The load distribution was determined through measurements conducted by the NC fire department. The distance between the front and back axle of the truck is 16 ft.

For each truck position along the bridge span, bridge deflection and longitudinal strains at mid-span

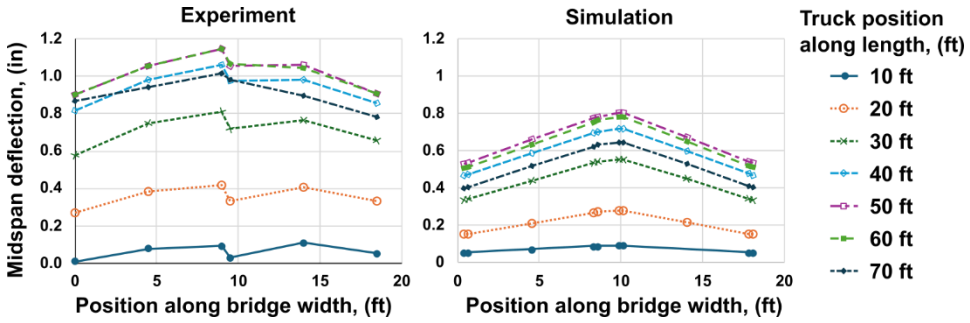

Figure 6: Experimental validation: models accurately predict the trends of bridge deflection under-predicting the magnitudes

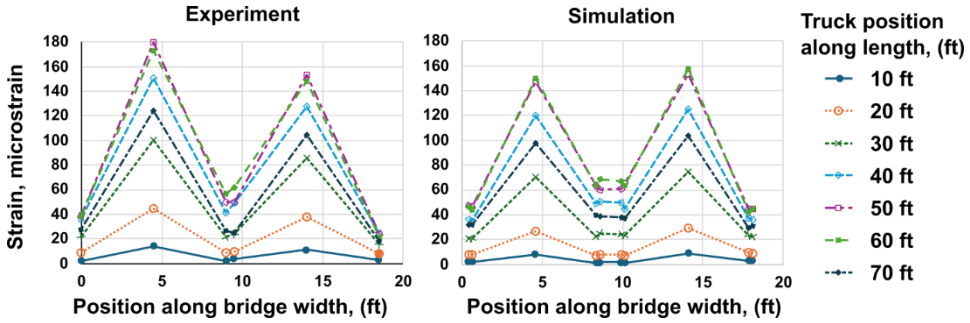

Figure 7: Experimental validation: strain trends from experiments and simulations are in good agreement

were extracted and compared to measured values. Note that displacements measured in the field test are referenced with respect to a 'zero' point that corresponds to the bridge's deflection under its own weight. Hence, for the purpose of model validation, experimental deflections are compared with live load displacements in the computational analysis.

Figure 6 shows the comparison between measured mid-span displacements and model predictions for each position of the firetruck along the bridge span. In this plot, the lines represent different truck positions, while the plotted points report bottom flange displacements at different points across the bridge width. Observe that both experimental and computational midspan deflections increase rapidly as the truck moves across the bridge (truck positions 10 ft, 20 ft, 30 ft and 40 ft). Maximum deflections are observed when the truck is nearly at mid-span (positions 50 and 60 ft). Similar trends are observed in longitudinal strains at the bottom flange, as shown in Figure 7. Strains increase as the truck approaches mid-span. Maximum strains occur for truck positions 50 ft and 60 ft, with values decreasing as the truck approaches the bridge end. It is also interesting to observe that the center of each railroad flatcar deck shows higher deflections and higher concentrations of strains suggesting that the central box plate girder carries most of the load. The maximum strain measured experimentally is 180e-6 which is well within the elastic limits (0.002).

While the computational displacement and strain trends mirror those observed experimentally, it is important to point out that the computational model reports lower displacements and strains compared to field data. The maximum measured mid-span deflection was around 1.1 inches, which the computational prediction is close to 0.8 inches. This is possibly due to the fact that the model boundary conditions prevent uplift at the bridge support, a phenomenon that was observed during the test. Furthermore, the test shows a difference in the vertical displacement measured in each of the two connected rail cars at the center plate, as can be seen in Figure 6. This discontinuity is due to the flexibility of the connection between the two cars and is not reflected in the computational model, where full compatibility is assumed. Strains are better predicted with a difference between computational results and field measurements of about 10%. The observation that strains show better agreement between test and model than displacements points to other sources of error, including small differences in truck position, measurement noise, or compliance in connections or support conditions.

In order to filter out potential sources of noise or compliance in absolute displacement measurements, we investigate trends in the relative displacement between the south car's center girder at mid-span and at a reference point on the same girder near the truck mount at the west end of the bridge. The experimental and computational differential displacements are shown in Figure 8 and display similar trends. Experimental results remain higher than model predictions. The difference, however, increases gradually as the truck approaches mid-span (truck position around 40 ft) and remains constant afterwards. This observation points to support uplift as the source of discrepancy since uplift is unlikely to happen when the truck is close to the west bridge end, increases gradually as it approaches the middle of the span, and remains constant afterwards.

As a side note, the numerical model shows a mid-span deflection of about 1.4 inches and strains of the order 250e-6 due to dead loads (self-weight of the bridge and 2 inches of asphalt). These values far exceed those measured under live loads, which is to be expected since the bridge weight far exceeds that of the firetruck. But since dead load effects are difficult to measure experimentally, numerical modeling can be instrumental for estimating design loads in structures such as railcar bridges, where simple calculations of weight demands are often not practical due to the complex geometry.

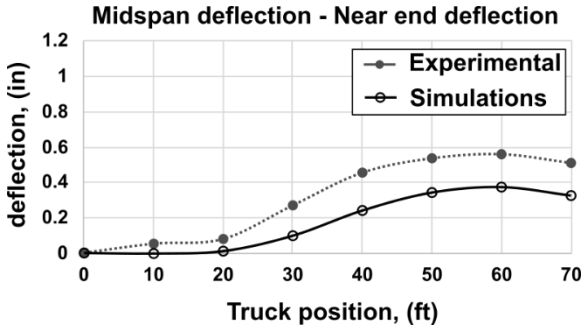

Figure 8: Differential in deflection between mid-span and reference end points in the south central girder

Chapter 4. Load Rating Methodology

Having established the fidelity of the computational model, we will now use it to compute load rating factors for the Warren Wilson bridge in Swannanoa. We will analyze the bridge for Emergency Vehicle 3 (EV3) loading. EV3 is a substantially higher load than the firetruck used for validation, and it is potentially critical for post-disaster relief. The truck will be positioned at center lane and will be moved along the bridge span to compute live load demand envelopes for load rating.

4.1. Live Load Application

EV3 is a truck with three axles carrying 24 and 31 kips on the front and each of the back axles, respectively, summing up to a total of 86 kips, according to NC legal loads. Per AASHTO guidelines, each axle is represented in the model by a rigid patch 20 inches wide and 10 inches long representing tires and separated by 6 ft, as shown in Figure 9. To simulate the truck passing over the bridge, the position of the truck along the span was varied in a step-by-step analysis for a total of 26 different positions. The first position corresponds to the truck approaching the bridge, with the front axle only positioned on the deck, and the last position representing the truck leaving the bridge, with the back axle load only applied to the deck.

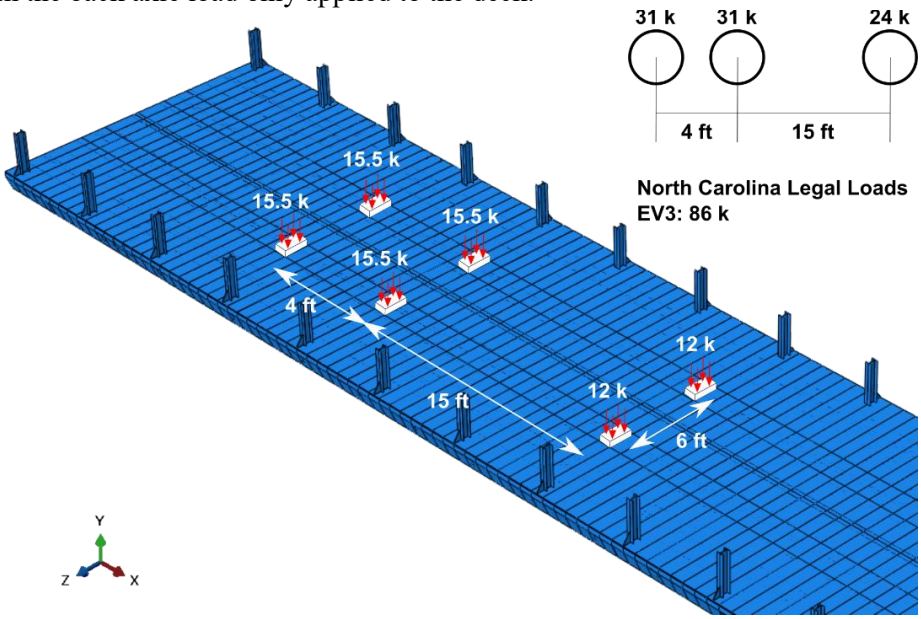

Figure 9: Load application: schematic representation of loads from NC Emergency Vehicle 3 used for load ratings

4.2. Bridge Division into Longitudinal Strips

As is conventionally done for load rating, the bridge is divided into strips that run along its span. Based on the railcar bridge geometry, we divide each railcar into central, internal, and external strips as shown in 10. In the 2D load rating, the overall load on the bridge is distributed to these strips using distribution factors specified by AASHTO. Each strip is then subjected to simplified two-dimensional (2D) analysis to assess demand and compute rating factors. With 3D

analysis results available, we can compute the demand on each strip from longitudinal and shear stress fields. We also extract section geometric properties to determine the members contributing to section capacity at each point, given the unconventional geometry.

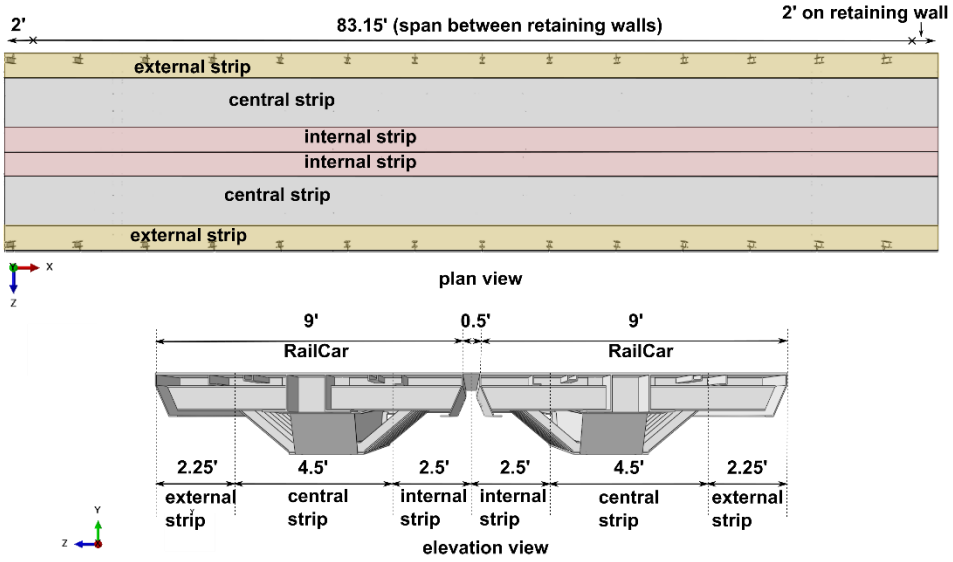

Figure 10: Plan and elevation view showing bridge divided into internal, central and external strips for analysis

4.3. Capacity and Demand Calculations

The computational model is used to extract cross-section geometry, stress, and strain data every 10 inches along the span, and for each truck position. Section properties, including positions of and dimensions of intersected members, are used to estimate section area and moment of inertia, while longitudinal and shear stress data are compiled using Python codes to estimate moment and shear demands, respectively. The process is described in more detail below.

4.4. Moment Capacity

The complex bridge geometry and changes in the configuration of structural elements cause the section capacity to be highly variable. For example, the moment capacity of the section where lateral braces are present would be higher than that of other sections. Conventional 2D analysis adopts the simplifying assumption that flanges of the central girder will resist all bending. The finite element model provides the opportunity to account for this variation in sectional geometry and compute the actual sectional capacity without making simplifying assumptions about load distribution.

Python codes were developed to compute the cross-sectional area of each section, its centroidal axis, and its second moment of inertia, thus enabling moment capacity computations at each section.

For each section, the bending capacity is calculated as

$$M_n = \frac{F_y * I}{y_{max}} \quad (1)$$

where,

M_n: nominal flexural capacity at location x along the length

F_y : steel yield stress y_{max} : distance of farthest fiber from centroidal axis, and

I_x : second area moment for the section

4.5. Shear Capacity

Similar to previous works ([4], [8]), we assume that girder webs carry shear loads. Web areas A_w at each section were computed manually from the known dimensions. The shear capacity at any section is given as

$$V_n = 0.6 * F_y * A_w \quad (2)$$

where,

V_n : nominal shear capacity at the section at position x along the span.

4.6. Moment Demand

As noted earlier, stresses and strains were extracted at sections at every 10 inches along the span. The geometry of the bridge changes continuously along the length and so does the stress distribution. The moment demand at each section is computed as the integration of the aggregate moment of normal stresses, computed as the product of normal stresses (σ) and centroidal distance (y), over the cross-sectional area.

$$M_{xx} = \int \sigma * y * dA \quad (3)$$

where,

M_{xx} : section bending moment demand at location x along the bridge span

σ : normal (longitudinal) stresses at a given point on the bridge cross-section

y : distance from the centroidal axis

dA : differential area.

4.7. Shear Demand

The shear demand at each section is computed as the integration of shear stresses (τ) over the cross-sectional area.

$$V_{xy} = \int \tau * dA \quad (4)$$

where,

V_{xy} : section shear demand at location x along the length

τ : shear stress.

4.8. Load Rating Factor

The AASHTO Manual for Bridge Evaluation (MBE) (2011)[9] sets criteria for load rating and posting of existing bridges for AASHTO design loads, state legal loads, or overweight permit loads. This work will follow the AASHTO provisions for load rating for state legal loads, as detailed below. The Load Rating Factor, (LRF) is defined as:

$$LRF = \frac{C - \gamma_{DC}(DC) - \gamma_{DW}(DW) \pm \gamma_P(P)}{\gamma_L(LL + IM)} \qquad (5)$$

where,

$C = \varphi_c\varphi_s\varphi R_n$; $(\varphi_c\varphi_s \geq 0.85)$

a_{ce} : is the condition factor accounting for deterioration of members, assumed 0.95 for poor condition

$\varphi_s = 0.085$ is the system factor for welded two-girder truss bridges

$\varphi = 1$ is the resistance factor for shear and flexure in steel (Table 6.5.4.2 of LFRD specifications)

We assume Load Factors for strength I Limit State, per table 6A.4.2.2-1:

$\gamma_{DC} = 1.25$

$\gamma_{DW} = 1.25$ (per 6A.2.2.3)

$\gamma_{LL} = 1.65$ per 6A.4.4.2.3a-1 assuming ADTT < 1000

DC is the Dead Load effect due to structural components and attachments

DW is the Dead Load effect due to wearing surfaces and utilities (asphalt)

P is the Permanent Load other than dead load (zero in the present case)

IM is the dynamic IMpact factor of 33% to account for dynamic impact of trucks

Thus, the LRF is computed as follows

$$LRF = \frac{0.85R\_n - 1.25(DC + DW)}{(1.65)(1.33)(LL)} \qquad (3)$$

For the purpose of this preliminary analysis, no reduction in cross-sectional area was assumed to account for corroded steep, as specified in MBE section 6.1.2.

Article 6A.2.1 of the MBE requires the consideration of permanent loads and vehicular loads in load rating only, thereby excluding other loads such as wind, ice, temperature, etc. Per article 6A2.3.2, since the roadway width is less than 18 ft, we consider only one lane of traffic and compute demand envelopes corresponding to one EV3 truck using 3D finite element analysis.

We also investigate the use of conventional 2D load rating procedures and compare results to rating factors obtained through 3D analysis. The goal is to estimate the role of three-dimensional behavior and stress distribution through different members on rating factors for railcar bridges.

4.9. 2D Load Rating

Typically, it is not practical to perform three-dimensional (3D) analysis on all bridges. AASHTO allows for the bridge system to be simplified and divided into strips as detailed in Section

3.2. For each section, a tributary width is assumed. The section capacity computations of each strip are simplified by identifying the effective area of the section that resists flexure and shear, respectively. For example, for the central strip, it would be assumed that flexure is primarily carried by the deck and flanges of the box plate, while shear is carried by the box plate girder web. These assumptions neglect the contribution of other members, such as braces, to the overall section capacity. The total live load on the bridge is assumed to be distributed to each strip in accordance with the distribution factors prescribed by AASHTO section 4.6.2. The distribution factors for moment and shear are computed differently.

The bridge was divided into strips as shown in Figure 10 for the purpose of 2D load rating. To keep the focus on identifying the effects of 3D load distribution on LRF, the 2D analysis will use the section capacity and dead load demand estimates computed using 3D FEM without accounting for factors such as tributary width and effective sections.

Live load distribution factors were computed per AASHTO section 4.6.2. It should be noted that these guidelines do not specify distribution factors for railroad flatcar bridges. The specifications for the'open steel grid deck on steel beam' bridge were decided to be most closely applicable to the railcar bridge. Per table 4.6.2.2.2b-2, the live load distribution factor per lane for moments in interior beams is S/7.5, where S is the spacing between beams, taken as 4.5 feet in the present bridge. All other distribution factors are computed by the lever rule per provisions of tables 4.6.2.2.- 2d-1, 31-1 and 3b-1. Also note that the lateral position of the truck was assumed to be at the center of the lane to be consistent with the 3D analysis.

Per the lever rule, the truck is placed at the center of the lane, and the internal and central beam take all the load when the truck is placed at the center of the lane. The distribution factor for external beams becomes zero for both flexure and shear. A multiple presence factor of 1.2 is used, considering a single lane of traffic.

Chapter 5. Results and Discussion

Figures 11 and 12 show the bending moment and shear force diagrams, respectively, for dead load and various positions of EV3. We can observe that the majority of the load is carried by the central girder as demands are significantly higher in the central strip. This pattern is also obvious in the bending moment and shear force envelopes shown in Figures 13 and 14. This result deviates from 2D analysis assumptions that attribute a larger portion of the load to internal girders. At the points where the cross-section changes (positions of lateral bracings, change of girder depth, etc.), there is a sudden change in the shear forces and bending moments carried by each strip. This shows that not only the box girders, but the complete section, including members like lateral braces, carry the load. This effect is well captured in the 3D FEM model and cannot be detected in conventional 2D analysis. 3D FEM results also indicate potential locations of stress concentrations occurring in the channel section flanges, and girder webs for flexure and shear, respectively, as shown in Figure 15.

Moment and shear demand envelopes are used to compute LRFs at each section. Note that, since capacity is not constant, lower rating factors are not necessarily correlated with higher demands. Tables 1 and 2 list the lowest load rating factors obtained using 2D and 3D analysis, as well as the location of the section for which these values are reported, identified by its distance from the western bridge support. We also compute the 3D LRFs obtained by analyzing the bridge as a whole entity or a single strip, for reference. Since the truck is placed at the center of the lane, the 2D analysis assumes the live load to be carried by the interior and central girders. Thus, LRFs for external girders are not applicable.

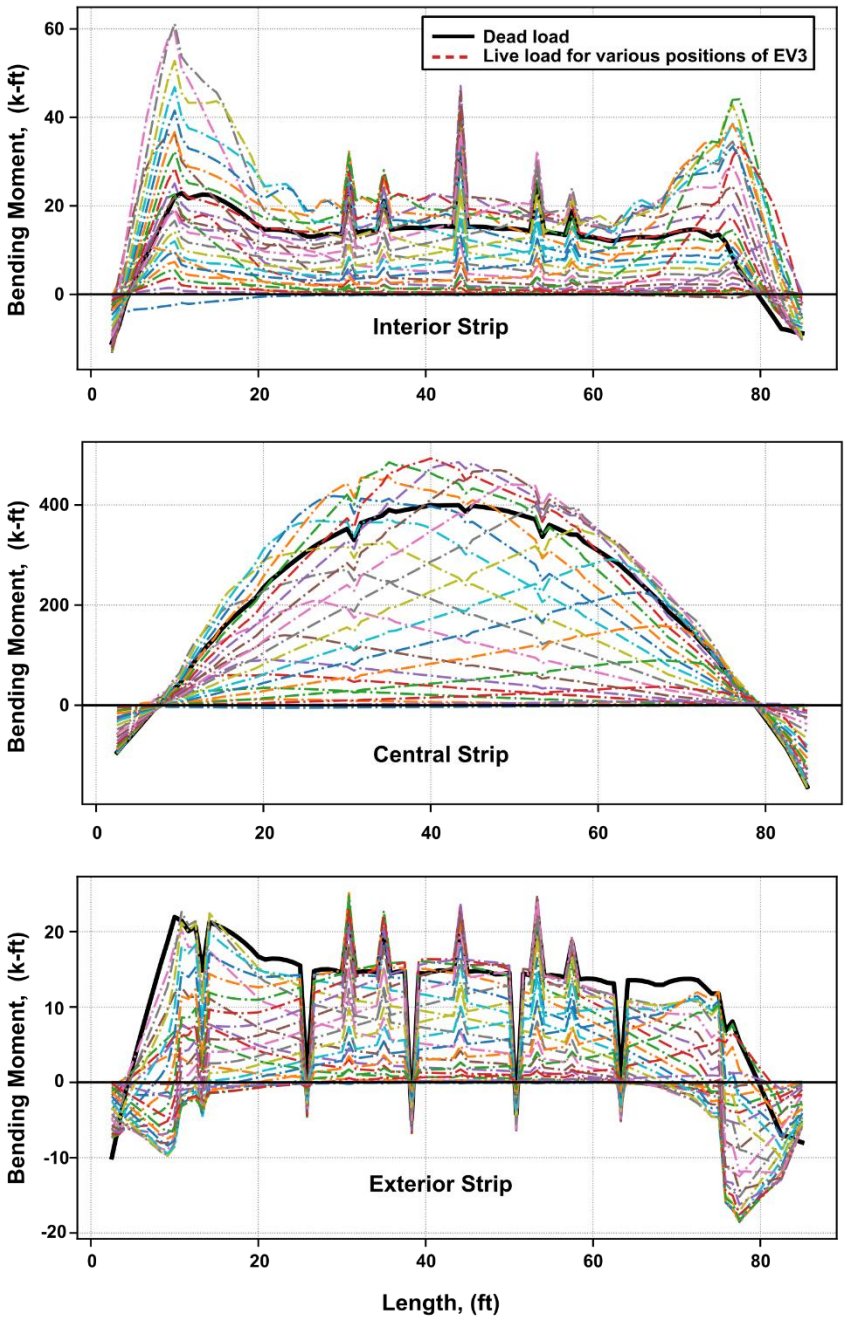

Figure 11: Bending moment diagrams for various EV3 truck positions

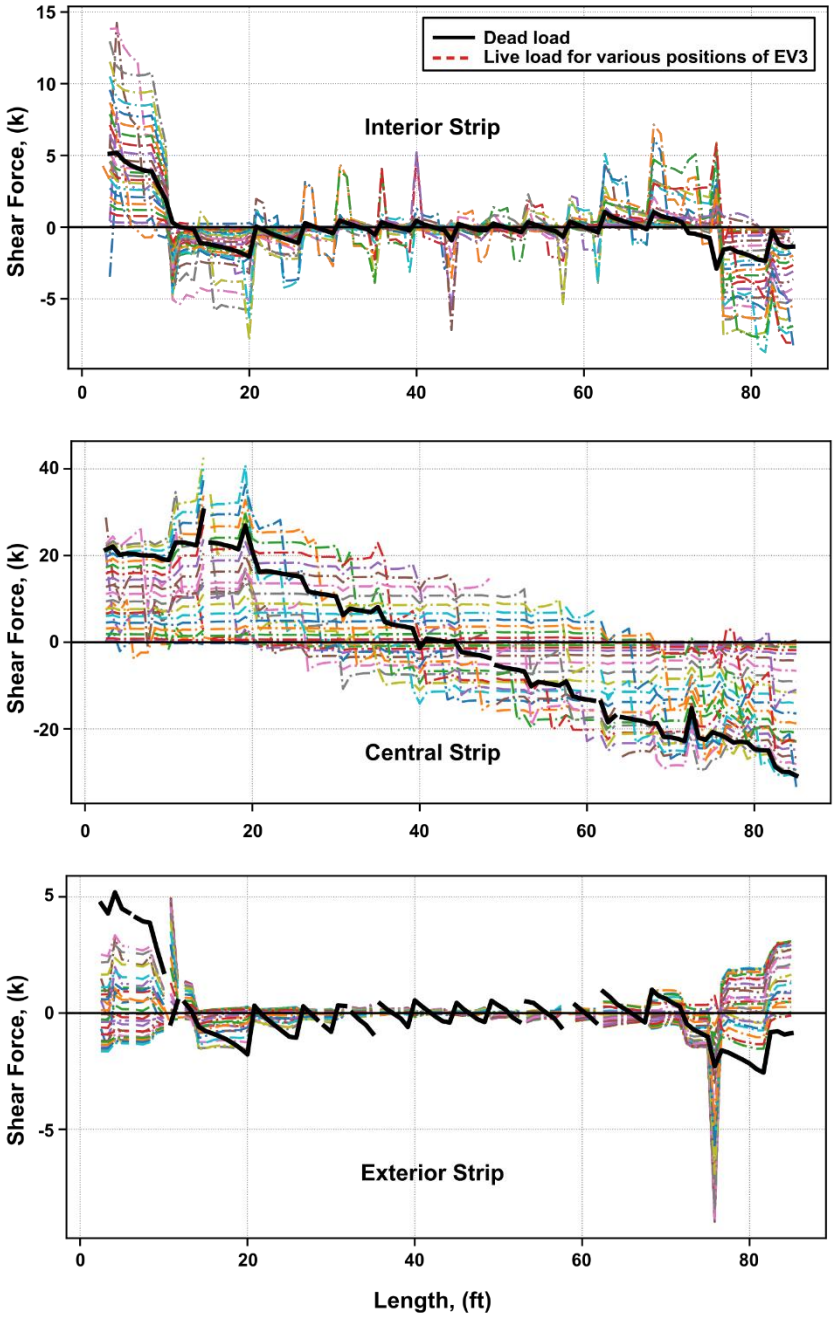

Figure 12: Shear force diagrams for various EV3 truck positions

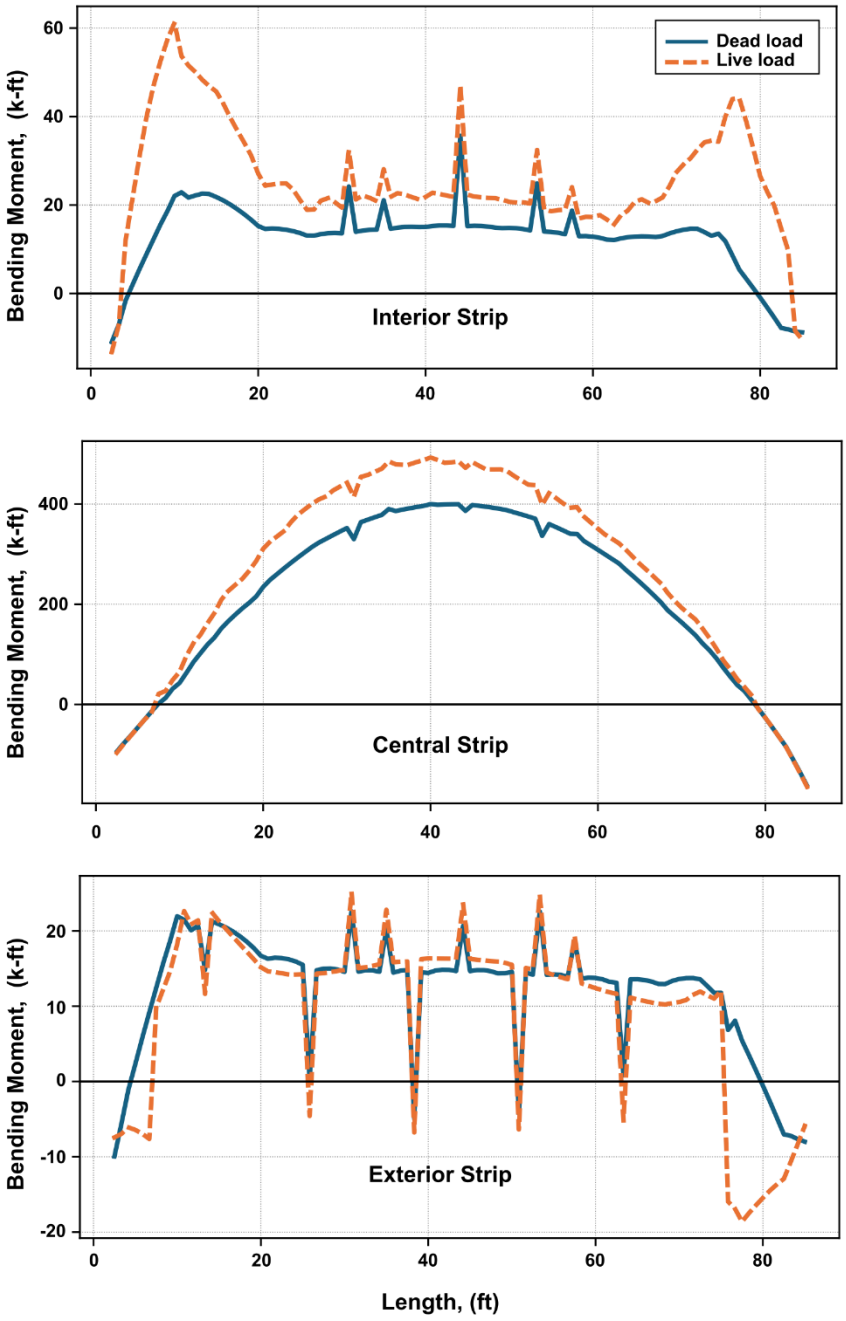

Figure 13: Bending moment envelopes

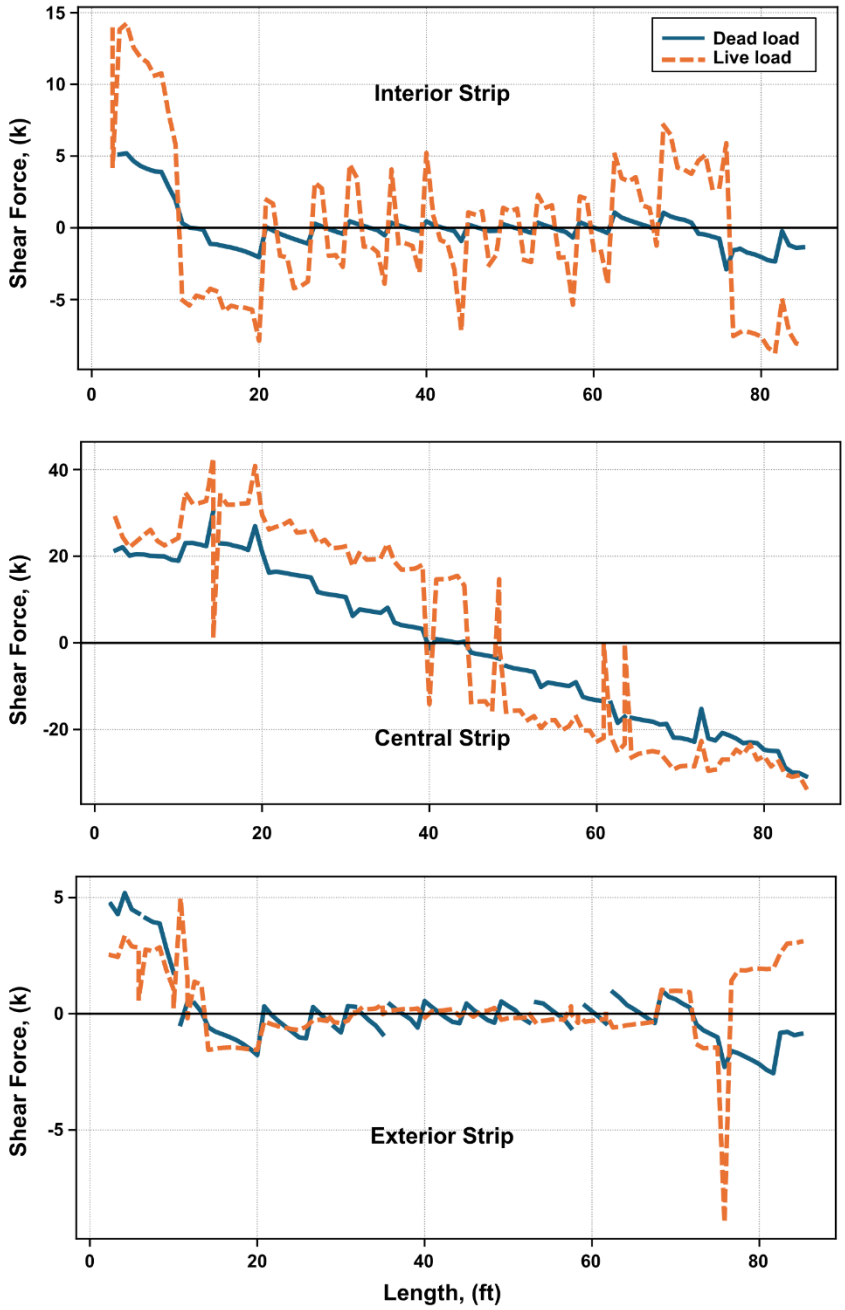

Figure 14: Shear force envelopes

	3D		2D	
Strip	**Min LRF**	**Dist.**	**Min LRF**	**Dist.**
Internal	0.65	7.2	0.04	38.0
Central	0.92	0.2	0.59	0.2
External	1.57	12.2	NA	NA
Continuous	0.93	38.0	NA	NA

Table 1: Flexure Results (3D vs 2D)

Flexure LRFs show vulnerabilities in the center and interior strips, with rating factors lower than 1. 2D rating factors are much more conservative compared to 3D, which indicates that a significant portion of the demand is distributed to the secondary elements. When the live load is in the center of the lane, simplified 2D analysis assumes the majority of the load to be distributed to the internal girder and the result indicates that this girder does not have sufficient flexural capacity, with a LFR of 0.04. 3D analysis, however, indicates that the majority of the load is allocated to the central girder, as seen in Figure 11. The central girder is the one that takes the most load. Thus, the 3D LRF for the internal girder is much higher than the 2D estimate. A similar trend is also observed in the LRFs for the central girder, with 2D distribution factors overestimating demand in the central strip due to not distributing load to the external strip. This leads to a significantly lower 2D LRFs for the central girder compared to 3D LRFs.

Furthermore, 3D strip-by-strip analysis suggests that the most critical sections are near the support (7.2 ft and 0.2 ft from the support), whereas 2D analysis indicates that the section close to mid-span (around 38 ft) in the internal girder is the most critical section. When the bridge is analyzed as a continuous entity, the flexure LRF increases to 0.93 for the section at mid-span. This LRFs is reflects the aggregate contribution of all structural members without assigned strip designations.

Although both 2D and 3D analyses show that the bridge is unsafe in flexure (LRF < 1), 3D analysis provides a more realistic assessment of bridge response and stress distribution compared to the overly conservative 2D LRFs.

Table 2 shows LRFs in shear and indicates that the bridge is safe, irrespective of the approach considered. It should be noted with caution, however, that the box girder webs of the box girder, considered to be the main shear carrying members, were fairly corroded, an effect not considered in this analysis.

	3D		2D	
Strip	**Min LRF**	**Dist.**	**Min LRF**	**Dist.**
Internal	2.79	2.2	1.26	0.5
Central	2.15	12.2	4.63	0.5
External	4.61	9.3	NA	NA
Continuous	4.15	12.2	NA	NA

Table 2: Shear Results (3D vs 2D)

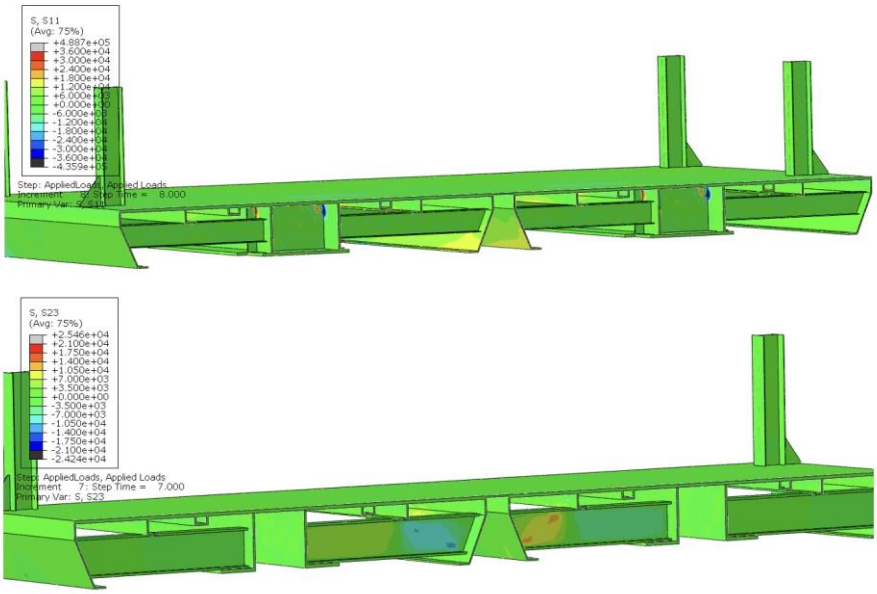

Figure 15: Normal (top) and shear (bottom) stress distributions

Chapter 6. Conclusions and Future Work

6.1. Conclusions and Future Work

The structural capacity of many temporary railcar bridges currently in use in WNC is largely unknown. This report establishes a methodology to compute Load Rating Factors (LRF) for railcar bridges using a detailed 3D physics-based finite element model. The model was validated using field test data and showed good agreement with results measured on site. Rating factors under EV3 rating revealed potential vulnerabilities in flexure, but further exploration is needed to assess bridge's maximum capacity. This exercise demonstrated that conventional 2D analysis significantly underestimates structural performance for load rating purposes and may lead to overly conservative load rating factors, resulting in high cost to the state.

Further research is needed to account for complex on-site conditions like local damages to the structural members, corrosion of members, and uplift at support. Analysis of a larger sample space would help establish a well-documented procedure for the quick assessment and deployment of temporary bridge structures in the state.

6.2. Recommendations

Analysis of the Swannanoa bridge considered in this study showed that the bridge is safe to operate with an emergency vehicle EV2, but can be consider unsafe with EV3, per NC legal loads.

A parametric study to quantify the effect of geometric parameters such as span, flatcar spacings along the width, number of flatcar etc on load rating results is recommended to build an inventory of temporary RRFC bridges for future use in NC.

6.3. Implementation and Technology Transfer Plan

The research team will work closely with the Structures Management Unit to plan for the implementation of these results. The methods developed herein will be implemented in a wider research effort supported by NC DOT1 to develop a load rating procedure for temporary railcar bridge structures and identify repairs or upgrades needed to existing railcars. The methods, tools, reports, and publications expected to be generated by this work would be available for broad use within and outside of North Carolina.

[1] Research Proposal 2027-066: “Load Capacity of Temporary Railcar Bridges in Western North Carolina” by Greg Lucier and Ghadir Haikal

References

[1] Richard Stradling for The News Observer. "'we got a bridge in 3 hours.' unusual material allows NCDOT to build fast after Helene'." Accessed 2025-11-01. [Online]. Available: https://www.newsobserver.com/ news/state/north-Carolina/article300876819.html.

[2] J. T. Provines, R. J. Connor, and R. J. Sherman, "Development of load rating procedure for railroad flatcar bridges through use of field instrumentation. i: Data collection and analysis," *Journal of Bridge Engineering*, vol. 19, no. 5, 2013. doi: 10.1061/(ASCE)BE.19435592.0000555.

[3] J. T. Provines, R. J. Connor, and R. J. Sherman, "Development of load rating procedure for railroad flatcar bridges through use of field instrumentation. ii: Procedure development," *Journal of Bridge Engineering*, vol. 19, no. 5, 2013. doi: 10.1061/(ASCE)BE.1943-5592.0000554.

[4] T. L. Washeleski, K. C. Sener, R. J. Connor, and A. H. Varma, "Load rating procedures for railroad flatcars repurposed as sustainable highway bridges," *Journal of Bridge Engineering*, vol. 21, no. 11, 2016. doi: 10.1061/(ASCE)BE.1943-5592.0000945.

[5] American Association of State Highway and Transportation Officials, *Aashto lrfd bridge design specifications*, 9th, Prepared by the AASHTO Committee on Bridges and Structures, AASHTO, Washington, DC, 2020.

[6] S. E. C. S. .-. WSP, "NCDOT railroad flatcar material testing data," Tech. Rep., 2025.

[7] Taylor Brodbeck, Vikita Kamala, and Gregory Lucier, "Load testing a temporary railcar bridge over bee tree creek in Swannanoa, NC," Tech. Rep., 2025, Released for NCDOT review.

[8] T. Washeleski, R. Connor, and J. Lloyd, "Laboratory testing of railroad flatcars for use as highway bridges on low-volume roads to determine ultimate strength and redundancy," Purdue University School of Civil Engineering, Tech. Rep. TR-2-2013, 2013, Manual, p. 273.

[9] AASHTO, *The Manual for Bridge Evaluation*, 3rd. Washington, D.C.: American Association of State Highway and Transportation Officials, 2018.

[10] K. Sener, T. Washeleski, and R. Connor, "Development of load rating procedures for railroad flatcars for use as highway bridges based on experimental and numerical studies," Tech. Rep., 2015, Manual, p. 80.

[11] NPR. "North Carolina lawmakers approve $600 m more for hurricane Helene recovery." Accessed 2025-11-01. [Online]. Available: https: //www.npr.org/2024/10/24/g-s1-29660/north-carolinahurricane-helene-damage.

[12] Parsons, T. J. (1990). Bridges constructed from railroad cars. In Second Workshop on Bridge Engineering Research in Progress, ProceedingsNational Science Foundation; Civil Engineering Department, University of Nevada. National Science Foundation; Civil Engineering Department, University of Reno.

[13] Wipf, T. J., Klaiber, F. W., Witt, J., & Threadgold, T. L. (1999). "Use of Railroad Flat Cars for Low-Volume Road Bridges," Iowa Department of Transportation Project TR-421. Iowa State University. August 1999.

[14] Wipf, T. J., Klaiber, F. W., & Doornink, J. D. (2003). "Demonstration Project using Railroad Flatcars for Low-Volume Road Bridges," Iowa Department of Transportation Project TR-444. Iowa State University. February 2003.

[15] Wipf, T. J., Klaiber F. W., Boomsma, H. A., & Palmer, K. S. (2007a). "Field Testing of Railroad Flatcar Bridges Volume I: Single Spans," Iowa Department of Transportation Project TR-498. Iowa State University. August 2007

[16] Wipf, T. J., Klaiber, F. W., Mass, J. J., Keierleber, B., & Witt, J. (2007b). "Field Testing of Railroad Flatcar Bridges Volume II: Multiple Spans," Iowa Department of Transportation Project TR-498. Iowa State University. August 2007.

[17] Sanayei, M., Reiff, A., Brenner, B., and Imbaro, G. (2015). "Load Rating of a Fully Instrumented Bridge: Comparison of LRFR Approaches." Journal of Performance of Constructed Facilities, 30(2), 4015019.